Null Test of Newton's Law at 100 μm

In string theories, the extra dimensions must be compactified, leaving the observed 3+1 spacetime dimensions. Unlike the other interactions, which are confined to the three space dimensions, gravity may escape into *n* gravity-only extra dimensions (see Figure 1), which could be as large as 0.1 mm [Arkani-Hamed *et al*., 1998]. For *n* = 2, the law of gravity should change from $1/r^2$ to $1/r^4$, as *r* is reduced to below R_2, the "radius of compactification". At $r > R_2$, the deviation is found to be:

$$\phi(r) = -\frac{GM}{r}\left[1 + \alpha \exp\left(-\frac{r}{\lambda}\right)\right]. \quad (1)$$

This is the first prediction of a string theory that can be tested, and a discovery of this deviation would be ground breaking!

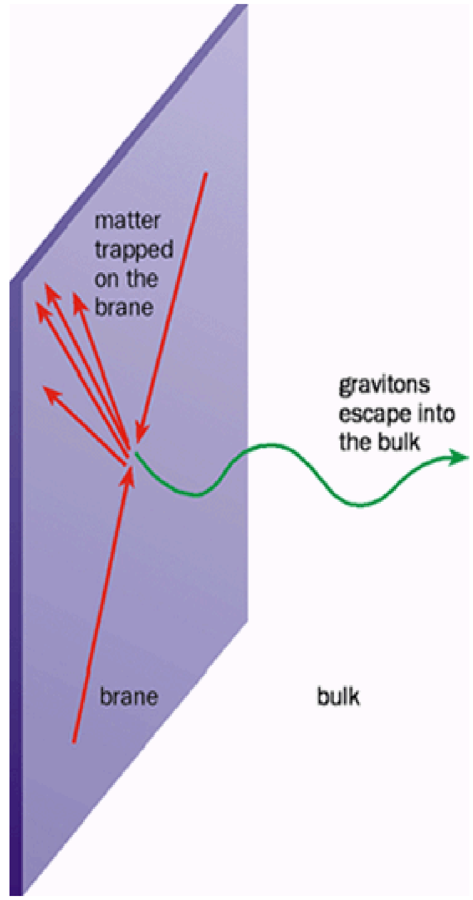

Figure 1. Gravity escapes into extra dimensions.

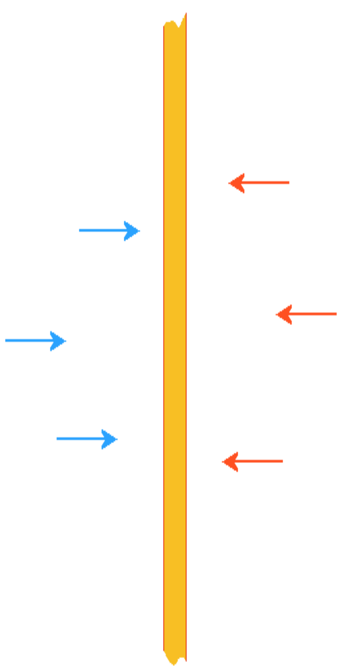

Figure 2. The Newtonian field due to an infinite plane slab of mass is independent of position.

Principle of the Experiment (UM1)

The principle of the null experiment is shown in Figure 2. The Newtonian field due to an infinite plane slab of uniform density is constant independent of position on either side of the slab. If a differential acceleration is measured between two test masses located on opposite sides of this source, the signal will remain constant as the source mass is displaced between them. On the other hand, any deviation from the $1/r^2$ law should result in a time-varying signal.

Experimental Apparatus

To approximate the null source, a circular disk of large diameter-to-thickness ratio is used. Two test masses, also disk-shaped, are suspended on opposite sides of the source at a distance of 280 μm from the surface. The experiment is cooled to 4.2 K to reduce the thermal noise and utilize superconducting technology.

Figure 3 shows an expanded cross section of the experiment. The entire housing is fabricated from niobium (Nb). The source is a tantalum (Ta) disk 1.59 mm thick by 165 mm in diameter, with mass 565 g. To minimize the mechanical cross talk between the source and detector, the source is suspended as a pendulum, free from the housing, and driven magnetically from the top of the cryostat. To be able to drive it with a small signal to a purely sinusoidal motion, the source is driven at its pendulum frequency, f_S = 0.47 Hz. The test masses are identical Nb disks 250 μm thick by 70 mm in diameter and are suspended by cantilever springs. Their dynamic mass is 8.7 g. The test masses are connected by a standard superconducting circuit [Moody *et al*., 2002] to form a differential

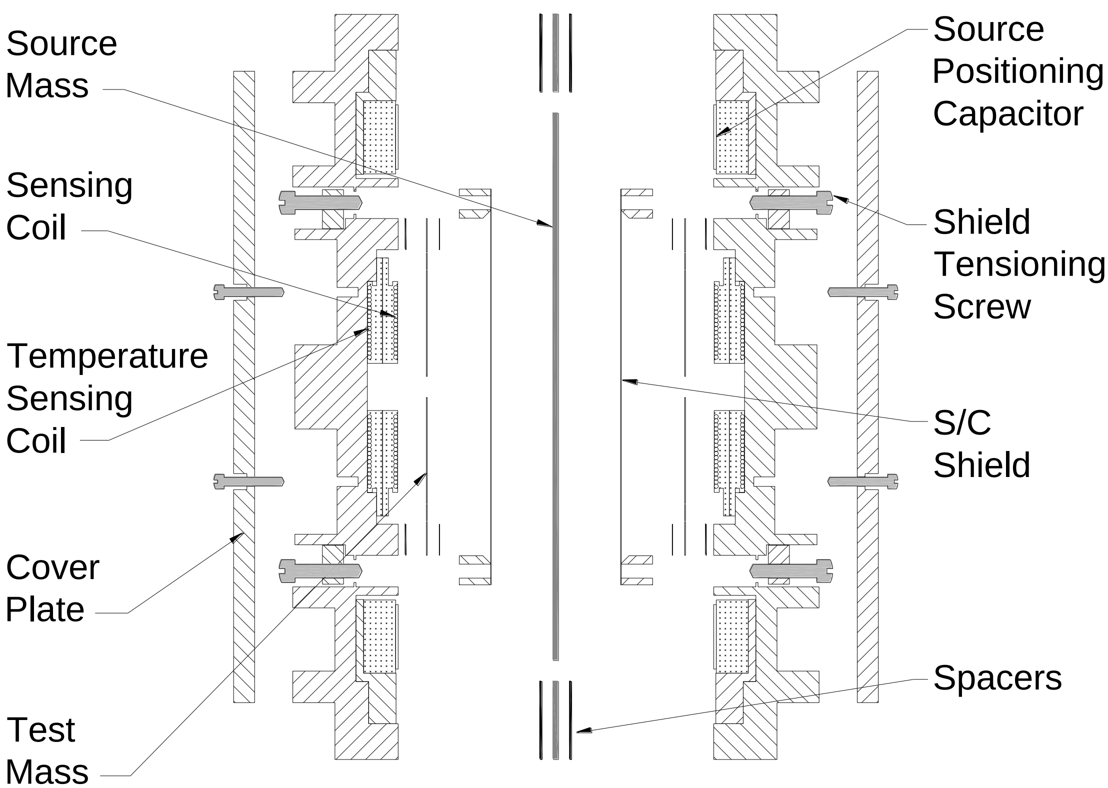

Figure 1. Expanded cross section of the experiment.

accelerometer. A 25-μm thick Nb foil provides electrostatic and magnetic shielding between the source and each test mass. The design allows a source displacement of ± 190 μm.

Expected Signal

The differential acceleration signals expected from the Yukawa force with $|\alpha| = 10^{-2}$ and $\lambda = 100$ μm are plotted in Figure 4 as a function of the source mass position. The Newtonian term arising from the finite source mass diameter is also shown. The source mass looks like an infinite plane slab to the test mass due to its proximity. The Yukawa signal is almost purely *second harmonic* to the source motion ($f = 2f_S = 0.94$ Hz), with an rms amplitude of 1.3×10^{-13} m s^{-2}.

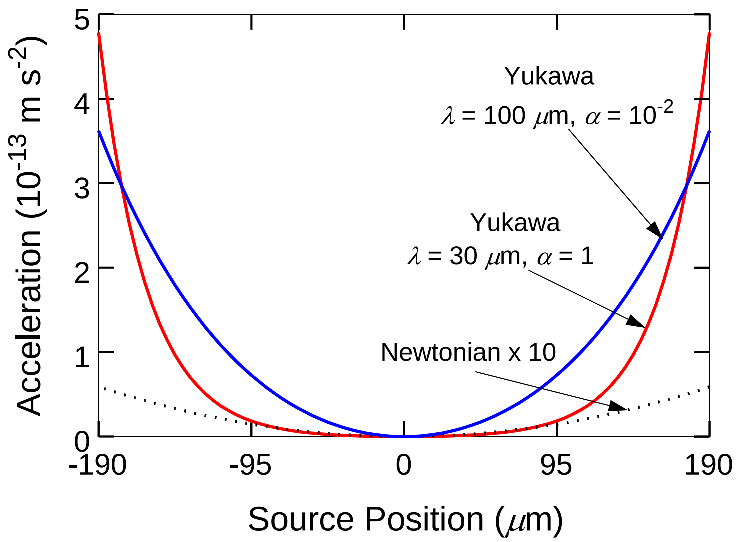

Figure 4. Newtonian and Yukawa signals versus source position.

Experimental Errors

For metrology, thickness errors dominate over density inhomogeneity due to the thin disk geometry of the source. The source mass is lapped to reduce the thickness errors to ≤ 10 μm.

The intrinsic power spectral density of a superconducting differential accelerometer is given by [Chan and Paik, 1987]

$$S_a(f) = \frac{8}{m}\left[\frac{k_B T \omega_D}{Q_D} + \frac{\omega_D^2}{2\eta\beta} E_A(f)\right], \qquad (1)$$

where m is the mass of each test mass, $\omega_D = 2\pi f_D$ and Q_D are the differential-mode (angular) resonance frequency and quality factor, β is the electromechanical energy coupling coefficient, η is the electrical energy coupling coefficient of the SQUID, and $E_A(f)$ is the input energy resolution of the dc SQUID. For our experiment, $T = 4.2$ K, $m = 8.7$ g, $f_D = 15$ Hz, $Q_D = 10^5$, $\eta = 0.25$, $\beta = 0.2$, and $E_A(f) = 1 \times 10^{-30}$ (1 + 0.1 Hz/f) J Hz^{-1}. This gives $S_a^{1/2}(f) = 1.2 \times 10^{-11}$ m s^{-2} $Hz^{-1/2}$ at f = 0.94 Hz. Assuming an integration time of 10^6 s, we find an rms noise of 1.2×10^{-14} m s^{-2}.

Error Source	Error	
	UM 1 ($\times 10^{-14}$ m s^{-2})	UM 2 ($\times 10^{-16}$ m s^{-2})
Metrology	0.3	0.5
Random (τ = 10^6 s)		
Intrinsic	1.2	3.3
Temperature	0.2	0.4
Seismic	0.7	5.2
Mechanical coupling	0.4	< 0.1
Magnetic coupling	< 0.1	< 0.1
Electrostatic coupling	< 0.1	< 0.1
Total	1.4	6.2

Table 1. Error budgets for UM1 and UM2.

Magnetic cross talk is an important error source. The isolation requirement for our experiment is 200 dB. We meet this requirement by combining a superconducting shield and frequency discrimination by second-harmonic detection. The patch fields, arising from potential differences across crystalline boundaries, produce forces between the source and the shields, and between the shields and test masses. These forces can produce a second-harmonic error through nonlinearities in the system. The Casimir force is not important in our experiment where gaps between conducting planes are ≥ 10 μm.

Table 1 combines all the errors of the experiment. The first column represents the present experiment with a distance-modulated source (UM1). The second column represents a future experiment with a density-modulated source (UM2), which will be described below.

Density-Modulated Source Experiment (UM2)

The $1/r^2$ law test using a distance-modulated source becomes increasingly difficult as the force range λ decreases. This is because such a source directly modulates parasitic forces such as from patch fields, the Casimir effect, and residual gas molecules. These problems could be alleviated if the source were to move laterally parallel to the shield, with its density modulated instead.

Figure 5 is the schematic of a density-modulated source experiment. Two spool-shaped masses made out of Nb are levitated by a current flowing through a single Nb tube. A Nb shield is placed between the masses to prevent direct electromagnetic cross-talks between them. Each mass carries two layers of source materials with high density contrast (Ta and Ti) on its surface facing the other mass. Each source layer is divided into $2n$ equal sections through which high and low density alternate. The density variation in one layer complements that in the other to keep the total areal mass density constant, thus producing a nearly constant Newtonian force as one mass rotates with respect to the other.

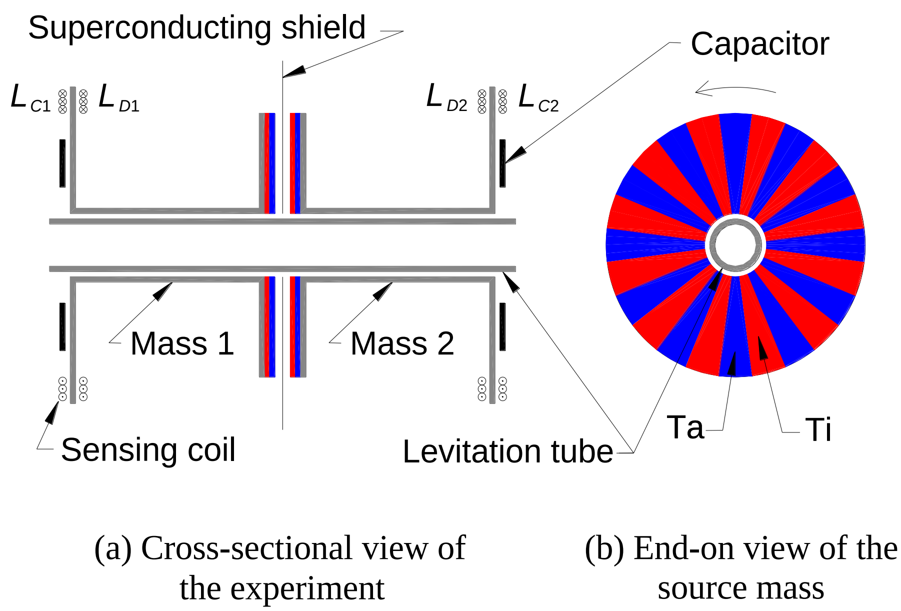

Figure 5. Schematic of a density-modulated source experiment with levitated masses (UM2).

To set up the levitation current along the tube, an N-turn wire is looped through the tube and a persistent current I_L is stored in this loop, as shown in Fig. 6(a). Then, due to the Meissner effect in a superconductor, a screening current $-NI_L$ is induced on the inner surface of the tube, which returns *uniformly* along the outer surface, independent of the wire geometry inside the tube. The magnetic field produced by the current NI_L on the outer surface of the tube levitates the source/test masses. Figure 6(b) shows how the displacement of the source/test mass perpendicular to the tube axis squeezes the field on one side and expands on the other, resulting in a restoring a force.

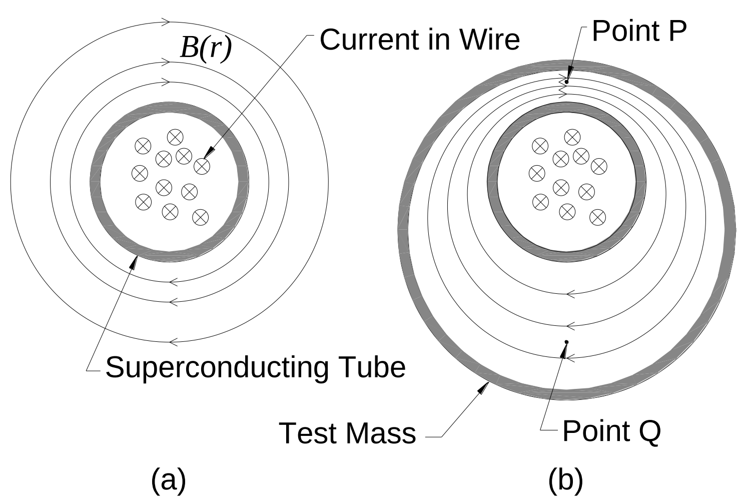

Figure 6. Principle of levitation by current induced on a superconducting tube.

At 4.2 K, a helium jet is introduced to spin up one of the masses about its symmetry axis and then pumped out, leaving the mass spinning with a very long decay time. Each mass acts as a source mass to the other, and a $1/r^2$ violation signal *would* appear as a differential acceleration at the n^{th} harmonic of the rotation frequency.

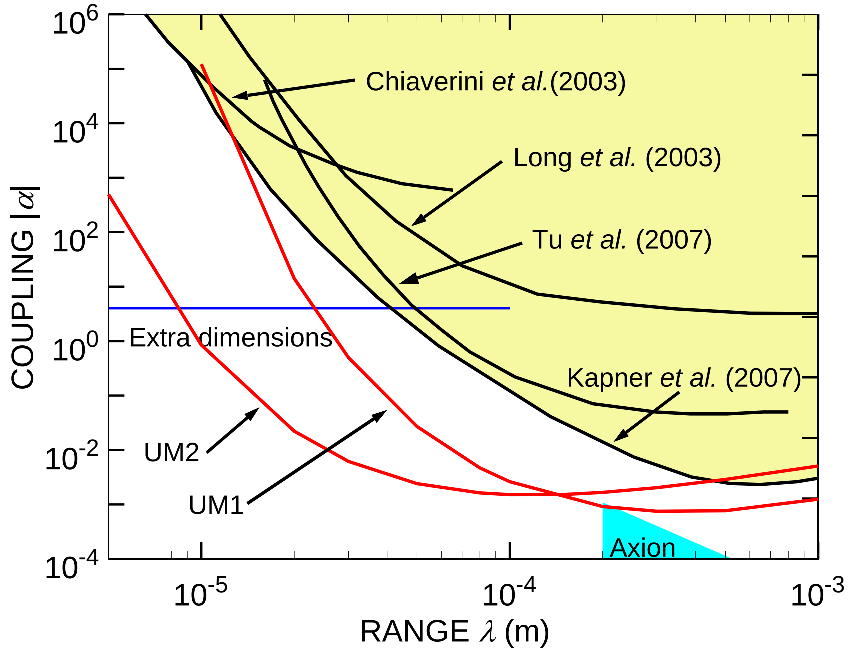

Figure 7. Expected resolution of UM1 and UM2 experiments.

Resolution of the Experiment

By equating the total error with the expected Yukawa signal, we compute the minimum detectable $|\alpha|$. Figure 7 shows the 2σ errors of UM1 and UM2 plotted as a function of λ, along with the existing limits [Chiaverini *et al*. 2002; Long *et al*., 2003; Tu *et al*,. 2007; Kapner *et al*., 2007]. The expected signals due to the string theory prediction and the axion [Moody and Wilchek, 1984] are also shown. The best resolution of UM1 is $|\alpha| = 5 \times 10^{-3}$ at λ = 300 μm. UM1 is expected to search for the extra dimensions down to R_2 = 25 μm. UM2 could extend the search to below 10 μm.

Arkani-Hamed, N., Dimopoulos, S., and Dvali, G. (1999), *Phys. Rev. D* **59**, 086004.
Chan, H. A. and Paik, H. J. (1987), *Phys. Rev. D* **35**, 3551.
Chiaverini, J. *et al*. (2003), *Phys. Rev. Lett*. **90**, 151101.
Kapner, D. J. *et al.* (2007), *Phys. Rev. Lett.* **98**, 021101.
Long, J. C. *et al.* (2003), *Nature* **421**, 922.
Moody, M. V., Canavan, E. R., and Paik, H. J. (2002), *Rev. Sci. Instrum.* **73**, 3957.
Moody, J. E. and Wilczek, F. (1984), *Phys. Rev. D* **30**, 130.
Tu, L.-C. *et al*. (2007), *Phys. Rev. Lett*. **98**, 201101.